Ultrasonics Sonochemistry 72 (2021) 105422

Contents lists available at ScienceDirect

Ultrasonics Sonochemistry

journal homepage: www.elsevier.com/locate/ultson

How do dissolved gases affect the sonochemical process of hydrogen production? An overview of thermodynamic and mechanistic effects – On the "hot spot theory"

Kaouther Kerboua [a,*], Slimane Merouani [b], Oualid Hamdaoui [c], Abdulaziz Alghyamah [c], Md. H. Islam [d], Henrik E. Hansen [d,e], Bruno G. Pollet [d]

[a] Higher School of Industrial Technologies, Department of Second Cycle, P.O. Box 218, 23000 Annaba, Algeria
[b] Laboratory of Environmental Process Engineering, Faculty of Process Engineering, University Salah Boubnider – Constantine 3, 25000 Constantine, Algeria
[c] Chemical Engineering Department, College of Engineering, King Saud University, P.O. Box 800, 11421 Riyadh, Saudi Arabia
[d] Hydrogen Energy and Sonochemistry Research Group, Department of Energy and Process Engineering, Faculty of Engineering, Norwegian University of Science and Technology (NTNU), NO-7491 Trondheim, Norway
[e] Electrochemistry Research Group, Department of Materials Science and Engineering, Faculty of Natural Sciences, Norwegian University of Science and Technology (NTNU), NO-7491 Trondheim, Norway

ARTICLE INFO

Keywords:
Hydrogen production
Sonochemistry
Dissolved gases
Thermodynamics
Mechanistic aspects

ABSTRACT

Although most of researchers agree on the elementary reactions behind the sonolytic formation of molecular hydrogen (H_2) from water, namely the radical attack of H_2O and H_2O_2 and the free radicals recombination, several recent papers ignore the intervention of the dissolved gas molecules in the kinetic pathways of free radicals, and hence may wrongly assess the effect of dissolved gases on the sonochemical production of hydrogen. One may fairly ask to which extent is it acceptable to ignore the role of the dissolved gas and its eventual decomposition inside the acoustic cavitation bubble? The present opinion paper discusses numerically the ways in which the nature of dissolved gas, i.e., N_2, O_2, Ar and air, may influence the kinetics of sonochemical hydrogen formation. The model evaluates the extent of direct physical effects, i.e., dynamics of bubble oscillation and collapse events if any, against indirect chemical effects, i.e., the chemical reactions of free radicals formation and consequently hydrogen emergence, it demonstrates the improvement in the sonochemical hydrogen production under argon and sheds light on several misinterpretations reported in earlier works, due to wrong assumptions mainly related to initial conditions. The paper also highlights the role of dissolved gases in the nature of created cavitation and hence the eventual bubble population phenomena that may prevent the achievement of the sonochemical activity. This is particularly demonstrated experimentally using a 20 kHz Sinaptec transducer and a Photron SA 5 high speed camera, in the case of CO_2-saturated water where degassing bubbles are formed instead of transient cavitation.

1. Introduction

According to the hot spot theory, sonochemistry is assumed as the indirect result of sonication of a liquid medium, this latter being the seat of acoustic cavitation events. The presence of dissolved gases is a sine qua non condition to the nucleation and the occurrence of acoustic cavitation and hence, the existence of sonochemical reactions [1]. Indeed, with no gaseous germs emerging within the liquid, the disruption of intermolecular bonds, which is the microscopic phenomenon behind acoustic cavitation, would require an enormous acoustic pressure of hundreds of bar [2]. Obviously, such an order of tensile strength to attain the nucleation threshold is impracticable and consequently, the only rationale for acoustic cavitation bubbles and sonochemistry based on the hot spot theory is gas dissolution, and hence heterogeneous nucleation [3].

The nature of the dissolved gas systematically acts on defining the cavitation and sonochemical thresholds and this implies, in addition the dissolved gas properties, the acoustic frequency, the acoustic amplitude and the ambient radius. The initial problematic treated in the present opinion paper can be simply formulated this way: in the presence of gaseous germs of the gas **X** , while applying an ultrasonic irradiation of a

* Corresponding author.
E-mail addresses: k.kerboua@esti-annaba.dz, kaouther.kerboua.esti@gmail.com (K. Kerboua).

https://doi.org/10.1016/j.ultsonch.2020.105422
Received 27 September 2020; Received in revised form 4 December 2020; Accepted 6 December 2020
Available online 24 December 2020

Nomenclature

α	Accommodation coefficient
ξ	Thermal layer width (m)
λ	Thermal conductivity (W/m·K)
ρ_L	Density of liquid (kg/m^3)
σ	Surface tension (N/m)
μ	Dynamic viscosity (Pa·s)
A	Area of the basis of the sonochemical reactor (m^2)
c	Sound celerity (m/s)
f	Frequency (Hz)
ΔH_i	Reaction heat of the ith reaction (J/mol)
m	Yield of evaporation and condensation (kg/m^2)
$\dot{m}$	Rate of evaporation and condensation (kg/m^2·s)
M	Molar mass of water (kg/mol)
n	Total molar yield (mol)
P	Acoustic power (W/m^3)
P_A	Acoustic amplitude (Pa)
P_i	Partial pressure (Pa)
P_g	Pressure of gas (Pa)
P_v	Saturating pressure (Pa)
P_∞	Ambient pressure (Pa)
Q	Heat (J)
R	Bubble radius (m)
$\dot{R}$	Bubble wall velocity (m/s)
$\ddot{R}$	Bubble wall acceleration (m/s^2)
r_i	Reaction rate of the ith reaction (mol/s m^3)
R_g	Ideal gas constant (J/mol·K)
S	Section of the bubble wall (m^2)
T	Temperature within the bubble (K)
t	Time (s)
T_∞	Ambient temperature (K)
V	Volume of the bubble (m^3)
V_R	Volume of the sonicated liquid in the sonochemical reactor (m^3)
W	Work (J)

frequency **f**, is the acoustic amplitude P_a sufficient to induce a subsequent growth of a bubble of an ambient radius R_0, or what is formally known as the cavitation threshold? The cavitation threshold is defined as the minimum amplitude of sound pressure required to initiate acoustic cavitation [4]. If expected to end-up to physical and chemical effects and then H_2 production, the cavitation should be inertial and active in sonochemistry. Curiously, in recent papers of Rashwan *et al.* [5,6], the sonochemical production of hydrogen at single acoustic cavitation bubble scale was investigated numerically under some unexpected conditions, namely an ambient radius of 1.5 μm, an acoustic amplitude of 0.1 MPa and an acoustic frequency of 20 kHz. The authors suggested a chemical scheme of 19 reversible reactions evolving within the bubble. The mechanism accounts for H_2O and O_2 cleavage, while the study exposes results under various saturating gases (O_2, air, CO_2, Ar, etc.), several values of extreme temperature (2,000, 4,000, 6,000, 8,000 and 10,000 K) and an extended time of 1,000 μs. What challenges us regarding the approach itself and these results is fundamentally the expected category of the bubble described earlier, according to its equilibrium radius under the adopted acoustic conditions [7], and consequently the unprecedented effect of dissolved gases allowing the achievement of the reported dramatic temperatures and considerable production of H_2. On the other hand, the quasi-agreement on the inhibition effect of CO_2 as a saturating gas on the sonochemical activity seems controverted [8–10]. These observations lead us to tackle a second problematic related to the validity of the assumptions leading to unprecedented results of sonochemical hydrogen production, and reiterate the question on how do dissolved gases affect the acoustic cavitation, sonochemistry and specifically H_2 production?

2. Thermodynamics and mechanistic aspects under Ar, air, N_2 and O_2 atmospheres: Illustrative cases and general guidelines

The starting points of the present opinion paper are the aforementioned conditions reported by Rashwan and coworkers [5], whilst the covered scope of ambient radii and acoustic amplitude will be extended to reach 60 μm and 0.12156 MPa, respectively. Assuming a single bubble of an equilibrium radius R_0, the initial composition of the bubble volume is expressed in terms of partial pressures as the sum of P_v and P_{g_0}. P_v refers to the vapor pressure of H_2O (the liquid medium is assumed as pure water) and is simply defined by any valid equation of liquid–gas equilibrium, while P_{g_0} is the pressure due to the saturating gas, given as indicated in Eq. (1).

$$P_{g_0} = P_\infty + \frac{2\sigma}{R_0} - P_V \tag{1}$$

Prima facie, the saturation with pure gas leads to similar initial conditions of bubble composition expressed in molar basis, in spite of the nature of the saturating gas. Volume based composition, however, is saturating gas dependent, since it accounts for the molar mass and the density.

The acoustic cavitation bubble oscillates according to the modified Keller-Miksis equation [11]. From a mechanical point of view and according to the ambient radius R_0 and the acoustic conditions f and P_a, the bubble can be dissolving, inertial or degassing [7]. The nature of the dissolving gas affects the bubble dynamics through the instantaneous gas pressure inside the bubble P and the mass rate $\dot{m}$ and acceleration $\ddot{m}$ of the non-equilibrium of evaporation and condensation of water molecules at the bubble interface, which depend at their turn of the partial pressure of H_2O and the temperature of the hot spot. The nature of dissolved gas clearly intervenes in a complex way on the bubble dynamics, the complex interactions are schematized in Fig. 1 (a) in an attempt to sum up the simultaneous evolution of the thermodynamic parameters.

We first present in Fig. 1(b) the bubble dynamics results under four different saturating atmospheres, namely air, N_2, O_2 and Ar, assuming a single bubble of 1.5 μm of equilibrium radius submitted to an ultrasonic wave of 20 kHz frequency and 0.1 MPa of acoustic amplitude. This non-exhaustive list of saturating gases serves as illustrative and comprehensive analysis to figure out some failures of approaches observed in the literature. As predicted, Fig. 1 (b) and (c) show that this scenario corresponds to a dissolving bubble rather than inertial with a growth ratio of barely 1.4. Physically, this means that the surface tension of water against the gas is still capable of braking the expansion of the bubble and preventing the expected explosive growth, hence, no dramatic temperatures are attained as shown in Fig. 1(c), and no hydrogen is produced! The causality relationship linking the bubble oscillation dynamics to the thermal behaviour and the sonochemical activity including H_2 production is further discussed below according to the saturating gas.

In order to observe the effects of dissolved gas on inertial and likely active bubbles in sonochemistry, we suggest to reach an inertial cavitation bubble, then a bubble active in sonochemistry under 20 kHz following two different pathways: (i) raising the bubble equilibrium radius, or (ii) increasing the acoustic amplitude. Since the study is intended for the sonochemical production of H_2, the discussion will

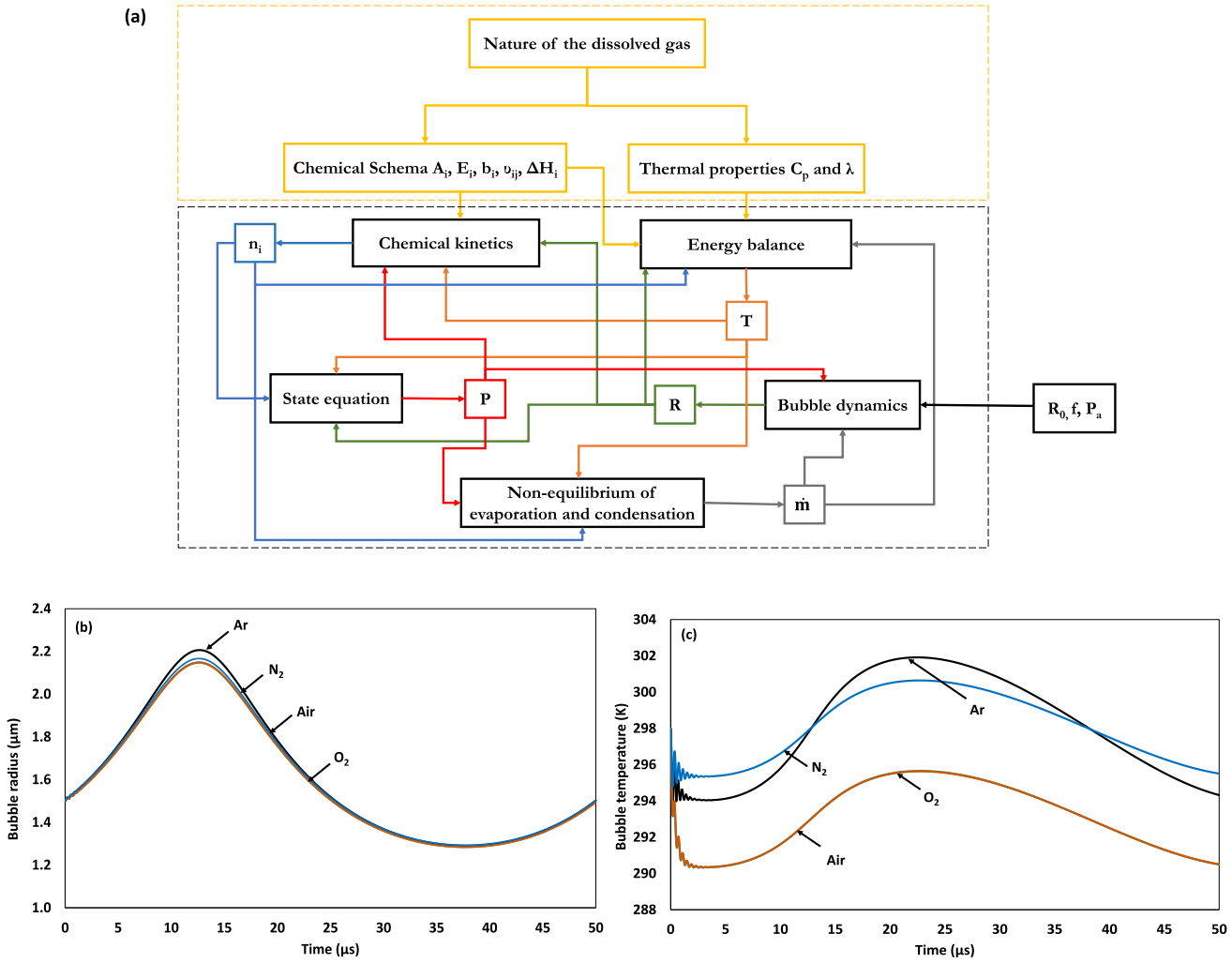

Fig. 1. Schematic diagram illustrating the complex effects of hypothesis related to the nature of the gas on thermodynamic and kinetic parameters (a) and illustrative dynamics (b) and thermal (c) results of an acoustic cavitation bubble having an equilibrium radius of 1.5 μm and submitted to an ultrasonic wave of 20 kHz frequency and 0.1 MPa, under four different saturating gaseous atmospheres.

emphasize on the sonochemical activity threshold for hydrogen production, fixed conventionally at a single bubble scale to 10^8 molecule·s·s^{-1} [7], which is equivalent to 8.3×10^{-21} mol of H_2 per cycle under 20 kHz.

Fig. 2 reports the bubble dynamics results and the corresponding temperature profiles under 0.1 MPa and 20 kHz in function of R_0 varying in the range (a): 1.5 μm, (b): 6 μm, (c): 10 μm, (d): 20 μm, (e): 30 μm and (f): 60 μm. It is firstly noticeable that while moving toward bigger bubbles at equilibrium, within the interval ranging from 1.5 to 60 μm, the motion of the bubble wall tends to demonstrate more pronounced bubble oscillation dynamics, though with expansion ratios limited to 2.5. This is accompanied of an increase of the temperature inside the bubble volume, until an order of 2700 K observed with bubbles having an ambient radius of 30 μm under an argon atmosphere. Interestingly, the first and strongest rebound of bubble oscillation always shows a harshest temperature condition within a medium saturated with argon, as compared to other saturating gases.

Fig. 3 represents the effect of the acoustic amplitude passing from 0.1 MPa ((a), (c), (e) and (f)) to 0.12156 MPa ((b), (d), (f) and (h)) on the bubble oscillation dynamics for two acoustic cavitation bubbles having respective equilibrium radii of 1.5 μm ((a) and (b)) and 60 μm ((c) and (d)) and their corresponding temperature profiles, as reported in Fig. 3 (e) and (f) for R_0 equal to 1.5 μm and Fig. 3 (g) and (h) for R_0 of 60 μm. The increase of the acoustic amplitude above the atmospheric pressure, with almost 21.6% relatively to the value adopted in Fig. 2, is equivalent to 47.8% supplementary consumption of acoustic energy according to Eq. (2).

$$P = \frac{P_a{}^2 A}{2\rho_L c V_R} \tag{2}$$

In terms of bubble wall motion, and according to Fig. 3 (a) and (b), a bubble of 1.5 μm, which is basically dissolving, knows a slight modification in growth ratio, passing from 1.4 to 1.9 under air, O_2 and N_2 atmospheres. Contrariwise, argon saturated liquid knows a higher expansion ratio of the bubble attaining 2.3. Although no severe compression is observed after the bubble growth and hence the bubble is still of dissolving nature, the advanced expansion of the bubble volume observed under argon, suggests a lower acoustic cavitation threshold in function of acoustic amplitude attained under this gas, as compared to other saturating gases. The corresponding temperature evolutions, reported in Fig. 3 (e) and (f), reveal profiles of dissolving bubbles, with remarkable micro-oscillations appearing under argon atmosphere. According to the nature of bubbles, and during the time interval corresponding to the bubble growth, the only implicated phenomenon is the mass transfer of water molecules, through the non-equilibrium of evaporation and condensation, dominated by evaporation.

Bubble with equilibrium radius of 60 μm was particularly selected as a second illustrative case to exhibit an interesting behavior. Fig. 3 (c)

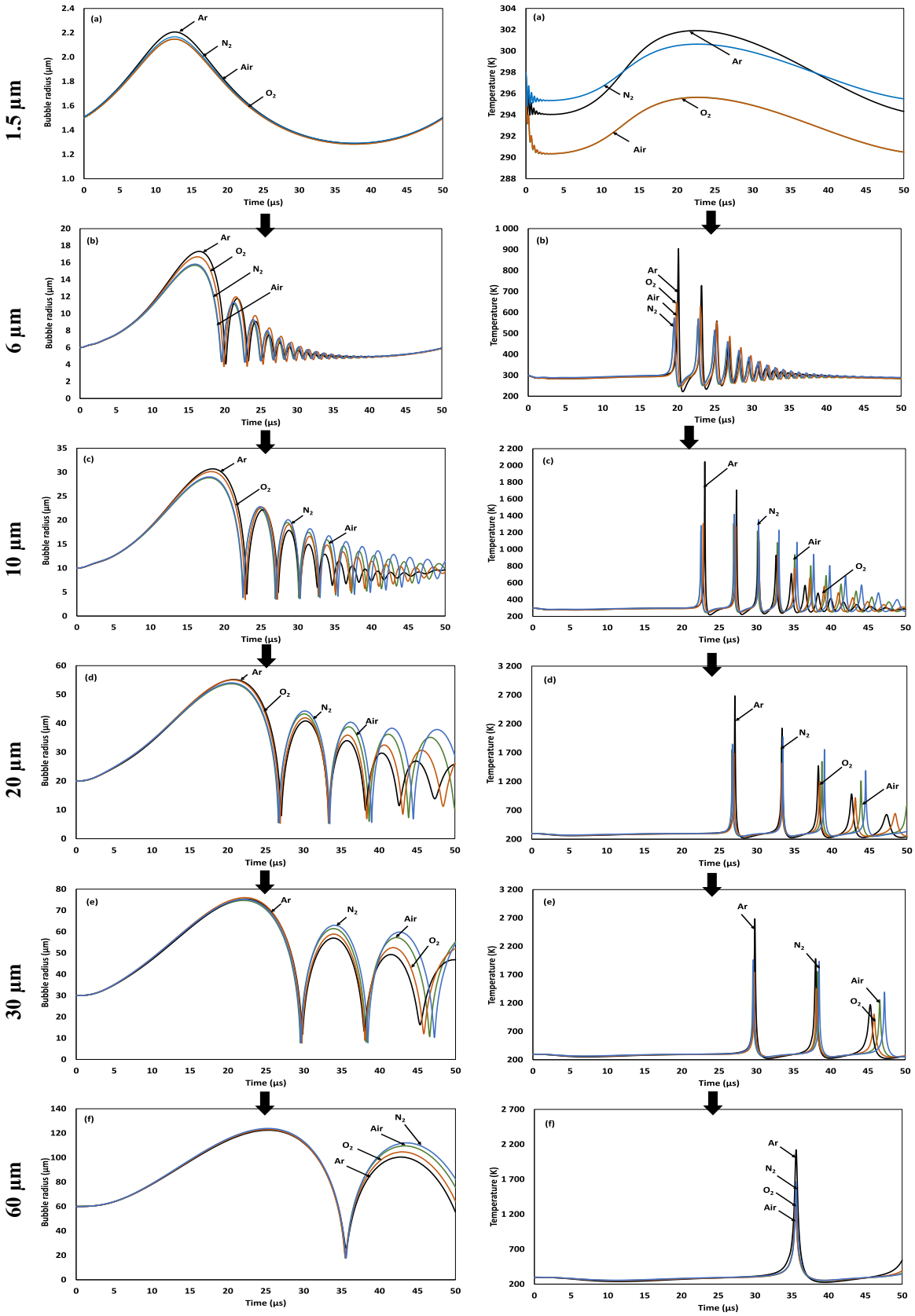

Fig. 2. Moving toward the sonochemical activity threshold for hydrogen production by the means of raising the equilibrium radius: Dynamics and thermal results of an acoustic cavitation bubble submitted to an ultrasonic wave of 20 kHz frequency and 0.1 MPa, under four different saturating gaseous atmospheres.

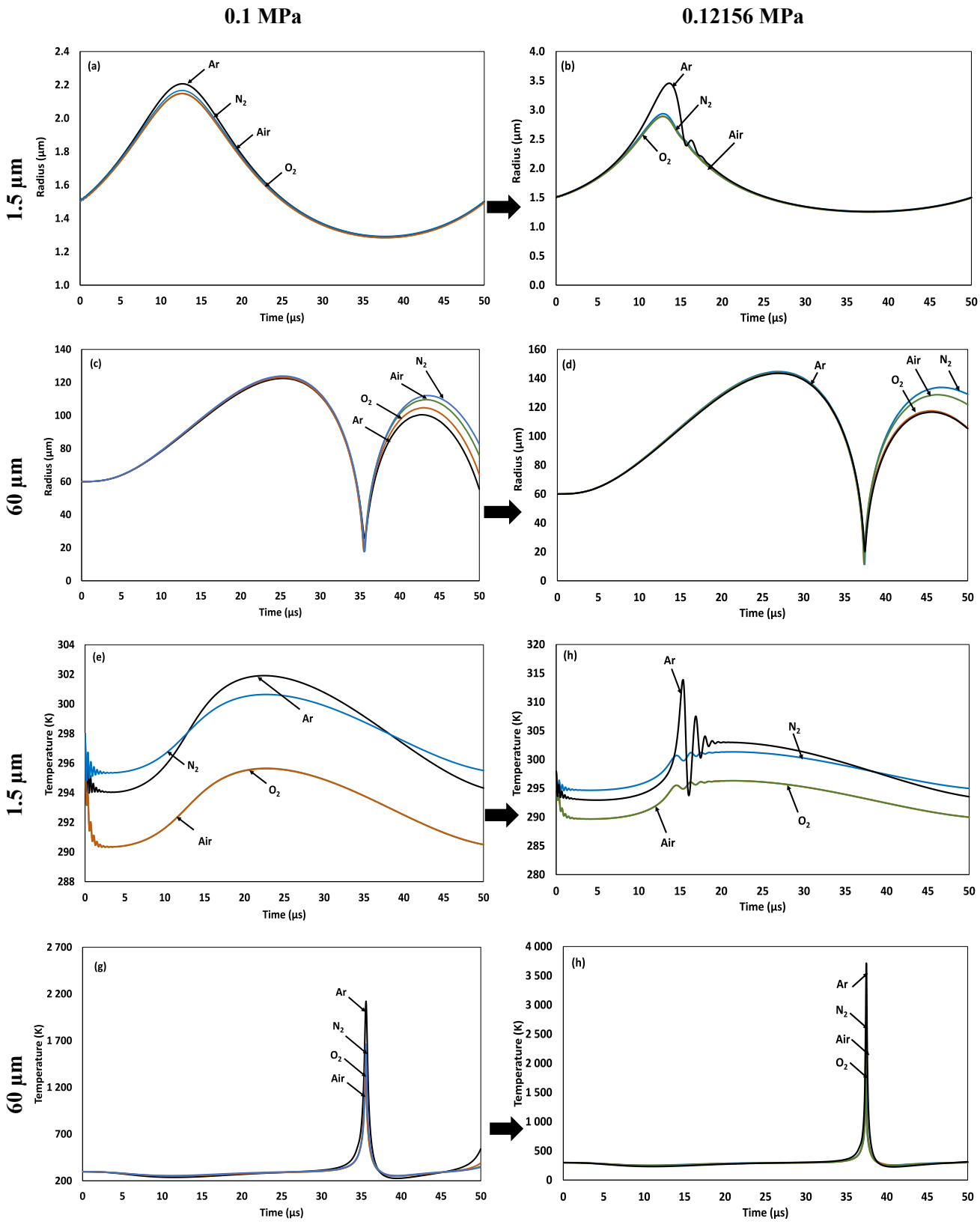

Fig. 3. Moving toward the sonochemical activity threshold for hydrogen production by the means of increasing the acoustic amplitude from 0.1 to 0.12156 MPa: Dynamics and thermal results of an acoustic cavitation bubbles having respective equilibrium radii of 1.5 and 60 µm and submitted to an ultrasonic wave of 20 kHz frequency, under four different saturating gaseous atmospheres.

and (d) demonstrate superimposed curves of bubble radius during the strongest expansion under the four saturating gases, with a common expansion ratio of 2 when the acoustic amplitude equals 0.1 MPa and 2.4 when it is raised to 0.12156 MPa. A clear strong compression is then observed in the four cases; however, the lowest compression ratio is recorded under an argon atmosphere. Indeed, with an acoustic amplitude of 0.1 MPa, the compression ratio is limited to 4.7 under Ar, while it increases to 6.8 under N_2 and O_2 and 7 under air. The augmentation of the acoustic amplitude to 0.12156 MPa induces a general increase of the compression ratios, with the lower value of 7.1 retrieved under argon, against 12.6, 11.8 and 12.8 under air, O_2 and N_2, respectively. Curiously, the corresponding temperature variations, reported in Fig. 3(g) and (h), demonstrate similar orders of hot spot temperature values in function of the saturating gas under both acoustic amplitudes of 0.1 and 0.12156 MPa. The highest value is recorded in the case of argon (2,097 and 3,710 K, respectively), followed by N_2 (1,652 and 2,720 K, respectively), then air (1,652 and 2,720, respectively) and finally oxygen (1,421 and 2,200 K, respectively). The nature of saturating gas may lead to less violent bubble compression but more extreme temperature conditions, as observed with argon. Mechanistically, the augmentation of temperature, which will be discussed later based on the energy balance, is responsible of braking of the condensation kinetics, according to the Hertz-Knudsen rate expressed in Eq. (3).

$$\dot{m} = \frac{\sqrt{M_{H_2O}}}{\sqrt{2\pi R_g}} \alpha \frac{1}{\sqrt{T}} (P_v - P_i) \tag{3}$$

Yet, no conclusion can be emitted regarding the sonochemical kinetics since both previous effects, i.e., the compression of the bubble volume and the collapse temperature, are opposed.

From an energetic point of view, the nature of dissolved gas governs the internal energy of the bubble through its heat capacity, the thermal loss across the boundary layer through the thermal conductivity, but also the heat capture or release related to the chemical reactions evolving within the bubble volume during collapse, and which are intrinsically dependent on the nature of the saturating gas and its eventual reactivity. Accordingly, the energy balance applied on the single acoustic cavitation bubble is directly impacted by the nature of the dissolved gas as shown in Eq. (4).

$$-P_g 4\pi R^2 \dot{R} - \frac{1}{3}\sum_{j=1}^{n} \Delta H_j r_j 4\pi R^3 + 4\pi R^2 \frac{\dot{m}}{M} C_{V_{H2O}} T = \frac{\lambda}{\xi} 4\pi R^2 (T - T_\infty) + \sum_{i=1}^{K} n_i C_{Vi} \dot{T} \tag{4}$$

The derivation of the energy balance from scratch would reveal some failure in the usually adopted models, but also clarify the extent of the effects of the saturating gas on the thermal behavior of the bubble. Basically, the first law of thermodynamics, stated in Eq. (5), applies to the single acoustic cavitation bubble.

$$\frac{dU}{dt} = \frac{\delta W}{dt} + \frac{\delta Q}{dt} \tag{5}$$

The substitution of the terms U, W and Q is based on the hypothesis governing the acoustic cavitation and its related phenomena, rigorously, their respective formulas are given in Eqs. (6), (7) and (8).

$$\frac{dU}{dt} = \sum_i n_i c_{vi} \frac{dT}{dt} + \sum_i h_i \frac{dn_i}{dt} \tag{6}$$

$$\frac{\delta W}{dt} = -P_g \frac{dV}{dt} \tag{7}$$

$$\frac{\delta Q}{dt} = -\frac{\lambda}{\xi} 4\pi R^2 (T - T_\infty) + 4\pi R^2 \frac{\dot{m}}{M} C_{V_{H2O}} T \tag{8}$$

However, most of studies tend to treat the bubble during collapse as a system with no mass variation and no heat exchange with the surrounding medium, thus, they limit the effect of dissolved gas to its polytropic index according to the Laplace equation and Mayer's relation [12]. Such an approach would not lead to realistic orders of magnitude of temperatures (exaggerated values) but may give acceptable insight into the increasing/decreasing order of attained temperatures according to the nature of saturating gas. In this case, the higher the polytropic index γ, the more important the expected temperature.

The more realistic approach includes the thermal conductive loss that accounts for the thermal conductivity of the saturating gas, the higher the thermal conductivity λ_g of the gas, the greater is the thermal loss by conduction and the lower the achievable temperature. It also involves the thermal exchange due to the physical kinetics, and simultaneously with the effect on the oscillation dynamics, the vapor condensation during collapse would reduce the internal energy of the bubble, partially governed by the specific heat capacity of the dissolving gas C_{v_g}, and consequently, the temperature decreases. Hence, the more intense the vapor condensation rate $\dot{m}$ and the higher the specific heat capacity of the saturating gas C_{v_g}, the lower the bubble temperature. Finally, the model comprises the reactions' heats ΔH_i, which closely depend on the reactivity of the dissolved gas and all the emerging species in its presence. However, one should regard into the orders of λ_g, C_{v_g}, ΔH_i and $\dot{m}$ if and only if the adopted model accounts for them, otherwise, the only valid basis of comparison is the polytropic index γ.

That's said, the adiabatic collapse model as adopted by Merouani *et al.* [8] and Rashwan *et al.* [5] would reasonably lead to a hot spot temperature under argon higher than under air; which is at its turn higher than under CO_2, owing to their respective polytropic indexes of 1.67, 1.4 and 1.3, given here at room temperature, but whose order remains applicable even at higher temperatures [13]. The present energy balance model, involving λ_g, C_{v_g}, ΔH_i and $\dot{m}$, would result in higher T_{max}under argon than under air and CO_2, owing to the increasing order of C_{v_g} and λ_g for Ar, air and CO_2, respectively [14]. The increase of temperature is expected to lower the condensation rate $\dot{m}$ and enhance the mutual effects on R and T_{max}, while the effects of ΔH_i proper to the reactional scheme related to the dissolving gas will be discussed jointly with the chemical mechanism. Anyway, the order of magnitude of temperature within the bubble volume under the precedent operational conditions, i.e. 0.1 MPa and 20 kHz, is far below the orders of magnitude announced in the recent published works, reaching 8,000 K [6], even if the ambient radius is increased beyond the dissolving zone, i.e. above 1.5 μm. Furthermore, it is clearly non-expectable to end up with the same order of bubble temperature if dealing with similar assumptions of f, P_a and R_0 while considering different saturating gases, especially when these gases are characterized by divaricated thermal properties, such as Ar, air and CO_2.

Besides, even if the inertial acoustic cavitation is assumed to occur, in respect to some conventional definitions based on expansion and abrupt compression [15], as indicated in Fig. 2(c) to (f) and Fig. 3(c) and (d), the sonochemical kinetics and particularly hydrogen production need to be assessed relatively to the sonochemical activity threshold, according to the saturating gas. Fig. 4 reports the sonochemical production of hydrogen associated to the cases presented previously in Fig. 2(c) to (f) and Fig. 3(c) and (d). Fig. 4(a), (b), (c) and (d) demonstrate that under 0.1 MPa, the nearest molar yield of hydrogen to the sonochemical activity threshold is encountered with a bubble of 30 μm of equilibrium radius oscillating under an argon atmosphere, it is estimated to 6.92×10^{-21} mol. With all the other cases, the produced yield of hydrogen does not exceed the order of 10^{-27} mol under N_2, 10^{-28} mol under air and 10^{-29} mol under O_2. With no surprise, a frequency of 20 kHz and an acoustic amplitude of 0.1 MPa are not expected to lead to a sonochemical activity of hydrogen production.

Fig. 3(e) and (f) indicate that the augmentation of the acoustic pressure to 0.12156 MPa induces a considerable increase of the yield of H_2, however, this augmentation is closely dependent of the saturating gas, and attains a molar yield of hydrogen beyond the sonochemical

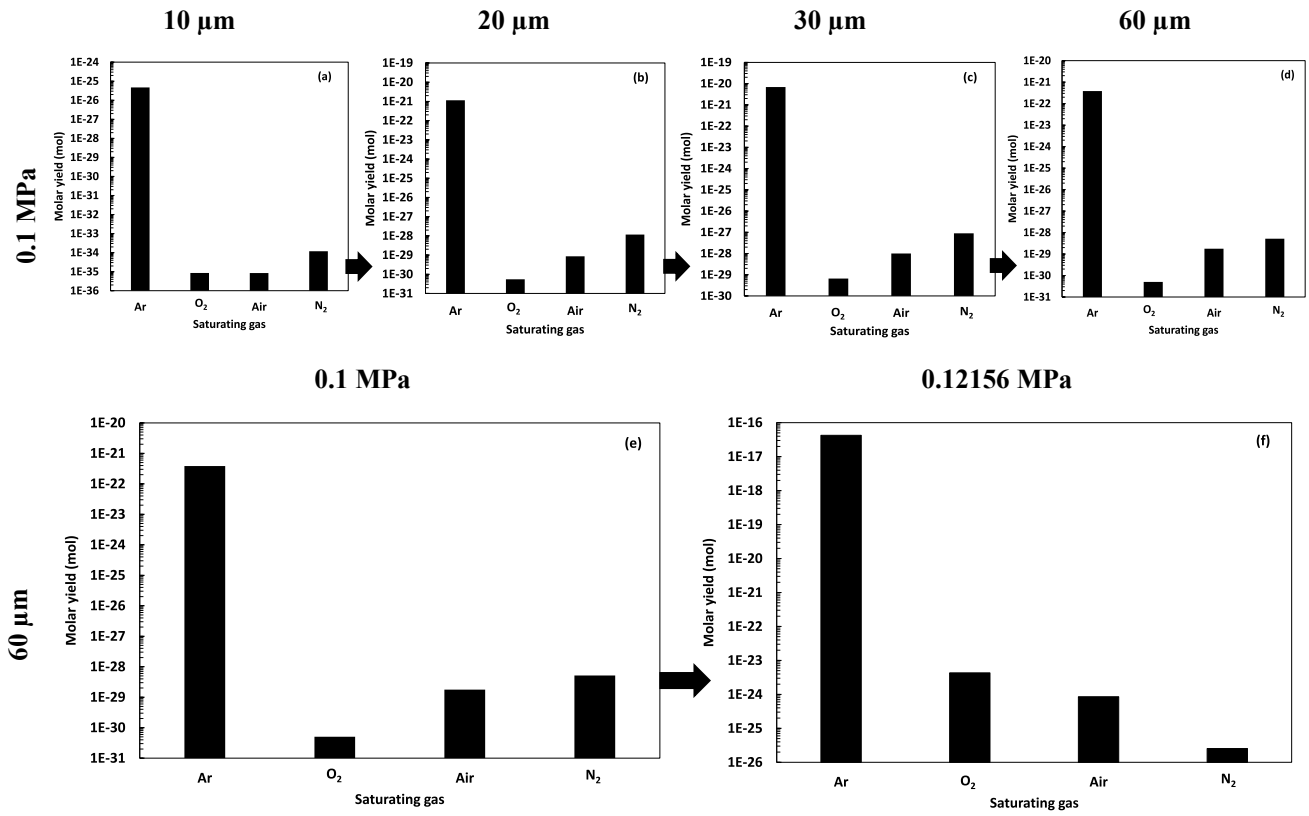

Fig. 4. H_2 production over one acoustic cycle under four different saturating gaseous atmospheres: Above and beyond the sonochemical activity threshold according to R_0 and P_a under an acoustic frequency of 20 kHz.

activity threshold only in the case of argon, with a value of 4.24×10^{-17} mol. The selective augmentation ratios in function of the dissolved gas are particularly interpellant and suggest a preferential formation pathway for hydrogen under argon, as compared to the other gases.

From a chemical mechanistic point of view, formation of hydrogen is mainly governed by the following elementary reactions ((9)-(12)):

$$H^{\bullet} + H^{\bullet} + M \rightarrow H_2 + M \quad (9)$$

$$H^{\bullet} + HO_2^{\bullet} \rightarrow O_2 + H_2 \quad (10)$$

$$H^{\bullet} + H_2O \rightarrow {}^{\bullet}OH + H_2 \quad (11)$$

$$H^{\bullet} + H_2O_2 \rightarrow H_2 + HO_2^{\bullet} \quad (12)$$

However, the nature of the dissolved gas implies supplementary reactions that completely change the kinetics of the four major pathways of hydrogen production within the acoustic cavitation bubble. We then propose to examine the reactivity of the saturating gas within the acoustic cavitation bubble and assess the likelihood of hydrogen formation based on the availability of hydrogen radical $H^{\bullet}$, which is the precursor of the four previous pathways (reactions (9)-(12)).

Under a pure oxygen atmosphere, $H^{\bullet}$ reacts with O_2, O and O_3 to form $HO_2^{\bullet}$ and $^{\bullet}OH$ according to the elementary reactions (13)-(16) [16]:

$$H^{\bullet} + O_2 + M \rightarrow HO_2^{\bullet} + M;\ \text{Coef. } H_2\text{: 2.5, } H_2O\text{:16.0} \quad (13)$$

$$O + H^{\bullet} + M \rightarrow {}^{\bullet}OH + M;\ \text{Coef}{\cdot}H_2O\text{: 5.0} \quad (14)$$

$$O_3 + H^{\bullet} \rightarrow HO_2^{\bullet} + O \quad (15)$$

$$O_3 + H^{\bullet} \rightarrow O_2 + {}^{\bullet}OH \quad (16)$$

The availability of $H^{\bullet}$ to form H_2 is mainly compromised by the emergence of $HO_2^{\bullet}$ and $^{\bullet}OH$, which are the two major sonochemical products within the oxygen bubble. Indeed, Kohno *et al.* [17] demonstrated using electron spin resonance-spin trapping method, that the saturation with O_2 conducts to the suppression of formation of $H^{\bullet}$, which reacts with oxygen to mostly form $HO_2^{\bullet}$.

Under a pure N_2 atmosphere, the N atom tends to scavenge the O atom through the reactions (17)-(23) [18]:

$$N_2 + O_2 \rightarrow N_2O + O \quad (17)$$

$$O + N_2 \rightarrow N + NO \quad (18)$$

$$O_2 + N \rightarrow O + NO \quad (19)$$

$$O + NO + M \rightarrow NO_2 + M;\ \text{Coef. NO: 20; Coef. O:20, } N_2\text{:20} \quad (20)$$

$$O_2 + N \rightarrow O + NO \quad (21)$$

$$HO^{\bullet} + N_2 \rightarrow N_2O + H^{\bullet} \quad (22)$$

$$HO^{\bullet} + N \rightarrow H^{\bullet} + NO \quad (23)$$

This implies higher availability of $H^{\bullet}$, to the detriment of $HO_2^{\bullet}$, which is the richest radical in O atom. In terms of hydrogen production, this compromises the second pathway of hydrogen formation through the elementary reaction (10).

In this context, Mead *et al.* [19] reported the preferential formation of nitric acid during the sonolysis of water saturated with nitrogen, this is due to the reaction (24).

$$HO^{\bullet} + NO_2 + M \rightarrow HNO_3 + M;\ \text{Coef. } N_2\text{:2} \quad (24)$$

The saturation with air is equivalent to the association of oxygen and nitrogen in respective molar proportions of 21% and 79%. The preceding reactional mechanistic effects are then accumulated. This was demonstrated by Merouani *et al.* [20] when studying the sensitivity of free radicals formation to the nature of the dissolved gas.

The saturation with argon is particularly interesting since Ar is inert and does not react with other species present within the bubble, it only

plays the role of the third body, which removes the excess of energy and stabilizes the chemical products according to the elementary reactions (25)-(31) [21].

$$H_2O + M \rightarrow H^{\bullet} + {}^{\bullet}OH + M;\ \text{Coef } H_2O\text{: 12, } H_2\text{:0.73, Ar: 0.38} \quad (25)$$

$$HO_2^{\bullet} + M \rightarrow H^{\bullet} + O_2 + M;\ \text{Coef } H_2O\text{: 14, } H_2\text{: 1.3, Ar: 0.67} \quad (26)$$

$${}^{\bullet}OH + M \rightarrow H^{\bullet} + O + M;\ \text{Coef } H_2O\text{: 12, } H_2\text{: 2.5, Ar: 0.75} \quad (27)$$

$$H_2O_2 + M \rightarrow {}^{\bullet}OH + {}^{\bullet}OH + M;\ \text{Coef } H_2O\text{: 12, } H_2\text{: 2.5, Ar: 0.64} \quad (28)$$

$$H^{\bullet} + O + M \rightarrow {}^{\bullet}OH + M;\ \text{Coef } H_2O\text{: 12, } H_2\text{: 2.5, Ar:0.75} \quad (29)$$

$$H^{\bullet} + O_2 + M \rightarrow HO_2^{\bullet} + M;\ \text{Coef } H_2O\text{: 14, } H_2\text{: 1.3, Ar: 0.67} \quad (30)$$

$${}^{\bullet}OH + {}^{\bullet}OH + M \rightarrow H_2O_2 + M;\ \text{Coef } H_2O\text{: 12, } H_2\text{: 2.5, Ar: 0.64} \quad (31)$$

In this case, the bubble is gaseous and argon is the predominant species in the bubble volume, the availability of the free radicals $H^{\bullet}$, $HO_2^{\bullet}$ and ${}^{\bullet}OH$, but also H_2O_2 is not compromised by the presence of any major species inside the bubble, and hence, the four pathways of the hydrogen formation are promoted. The beneficial effect of argon on the sonochemical activity was previously pointed out by Wayment and Casadonte [22] and Kohno et al. [17].

By extrapolation, the saturation with CO_2 engenders a mechanism recombining the C atom to the free radicals available in the medium, this generates species such as HCO, COOH and CH_2O (10^{10} to 10^{14} $cm^3{\cdot}mol^{-1}{\cdot}s^{-1}$ and $cm^6{\cdot}mol^{-2}{\cdot}s^{-1}$), with high scavenging effects of $H^{\bullet}$ and O, as shown in the elementary reactions (32)-(36) [8].

$$CO_2 + M \rightarrow CO + O + M \quad (32)$$

$$CO_2 + H^{\bullet} \rightarrow CO + {}^{\bullet}OH \quad (33)$$

$$CO_2 + H^{\bullet} \rightarrow COOH \quad (34)$$

$$CO + H^{\bullet} + M \rightarrow HCO + M \quad (35)$$

$$HCO + HCO \rightarrow CH_2O + CO \quad (36)$$

The dissolving gas, if not inert, is a full-fledged reagent in the sonochemical mechanism, its role is not limited to that of the third body, and its reactivity may give rise to sub-products, which scavenge the needed species for hydrogen emergence. One of the major failures of the numerical models describing the sonochemical activity, and hence the sonochemical production of hydrogen, is ignoring the side reactions of the saturation gas.

The acoustic cavitation bubble, if active, represents a unique chemical reactor model with some specifications that should be considered when undertaking the modeling of the sonochemical activity at single bubble scale and before tackling the effects of the saturating gas on the sonochemical production of hydrogen. In the case of this particular microscopic reactor, the reaction or residence time is an intrinsic parameter that depends simultaneously of the oscillation dynamics and the energy balance applied on the bubble volume, that define the infinitesimal time slot during which dramatic temperature and pressure conditions occur and induce chemical interactions. This time slot manifests once per acoustic period and is repeated during the bubble lifetime at the number of cycles that take place during the irradiation time. The rapid evolution in temperature, pressure and volume surrounding the bubble collapse requires simultaneous simulation of chemical kinetics and thermodynamic parameters variation versus time. One should carefully define the "reactional conditions" and rigorously resolve the sonochemical kinetics model, since once again; the acoustic cavitation bubble is a unique microscopic reactor model with instantaneously varying conditions.

Finally, it is worthy to pay readers attention to a key aspect that may further orientate the effects of the saturating gases on the sonochemical activity and hydrogen formation, which is the dependency of the equilibrium size of the acoustic cavitation bubble of the dissolved gas nature and its solubility in water. The equilibrium radius of the bubble is the result of the static mechanical equilibrium at the bubble interface governed by the formula [23]:

$$P_v(T_\infty) + \frac{m_g R T_\infty}{M_g \frac{4}{3}\pi {R_0}^3} - \frac{2\sigma}{R_0} = P_\infty \quad (37)$$

The ambient radius of a free spherical gas bubble in a quiet liquid is clearly dependent of the nature of the dissolved gas, which questions the initial size of the gaseous bubble under the effect of an ultrasonic field.

In an early paper, Henglein [24] pointed out that generally, the sonochemical activity takes place only in the presence of a mono or diatomic gas in the irradiated solution. The author demonstrated that cavitation produces gas bubbles, and the chemical effects depend on the nature of the gas. According to his earlier study [25], polyatomic gases such as CO_2 can only be introduced in few percentage within mono or biatomic matrix to expect a sonochemical effect. This is explained by the fact that, in case of high concentration, gas bubbles are not in Henry's equilibrium with the surrounding aqueous gas solution. Besides, Harada and coworkers [26] proved that under pure CO_2 atmosphere, no sonochemical products are detected. They attributed that to the restrained cavitation by dissolved CO_2. The same research group elaborated several studies on the sonolytic reduction of CO_2 in water [27,28], they demonstrated that the addition of CO_2 with very low proportions (2% to 3% molar) to an argon matrix dissolved in water induces an enhancement of KI oxidation. This observation was explained by the high solubility of CO_2 that improves the concentration of cavitation nuclei. However, at higher concentration, the drastic increase of the number of nucleation sites would elevate the likelihood of bubble coalescence during sonication, the sonochemical effect is consequently inhibited. This explanation is further supported by the images captured by Rooze *et al.* [29] of the bubble fields under air and carbon dioxide using a light source. In the present opinion paper, it is suggested that, due to its high solubility, CO_2 tends to form bigger bubble at equilibrium than other gases, their oscillation under the effect of an ultrasonic field is then expected to lead to degassing bubble, as demonstrated by Yasui [7]. This suggestion is investigated experimentally in the following section using high speed camera records.

3. Experimental insights

In the present section, some experimental insights are given in terms of the visualization of acoustic cavitation bubbles under several dissolved gases, in order to inspect the nature of formed bubbles and examine the effect of the population behaviour on the preconized sonochemical hydrogen production. The experimental procedure presented here aims to complete the view intended by the opinion paper rather than setting an independent experimental investigation. In the experimental procedure, a 20 kHz Sinaptec transducer placed at the bottom of 1 L cylindrical vertical reactor of 6 cm of diameter was used. Different gases, namely O_2, N_2, Ar and CO_2, were injected from the lower inlet of the reactor into a volume of 400 mL of pure water during 20 min. After 20 min of bubbling, the reactor was closed completely. The sonication was then performed at 50% acoustic amplitude for 30 s and images were captured using a high-speed camera (Photron SA 5 camera) at 5,000 fps (frame per second). The visual observation of the cavitation phenomena under different saturation gases were captured through the high-speed camera and presented in Fig. 5. The different dissolved gases resulted in very prominent difference in terms of cavitation activity. This is particularly noticeable in the case of CO_2-saturated water; indeed, the captured image demonstrates the apparition of large gas bubbles when sonicating CO_2-saturated water, which indicates that mainly degassing bubbles are formed and degasification of the dissolved CO_2 occurs instead of transient cavitation active in sonochemistry. Some degasification can also be observed under O_2 atmosphere while very few degassed bubbles were observed under N_2. However, the captured

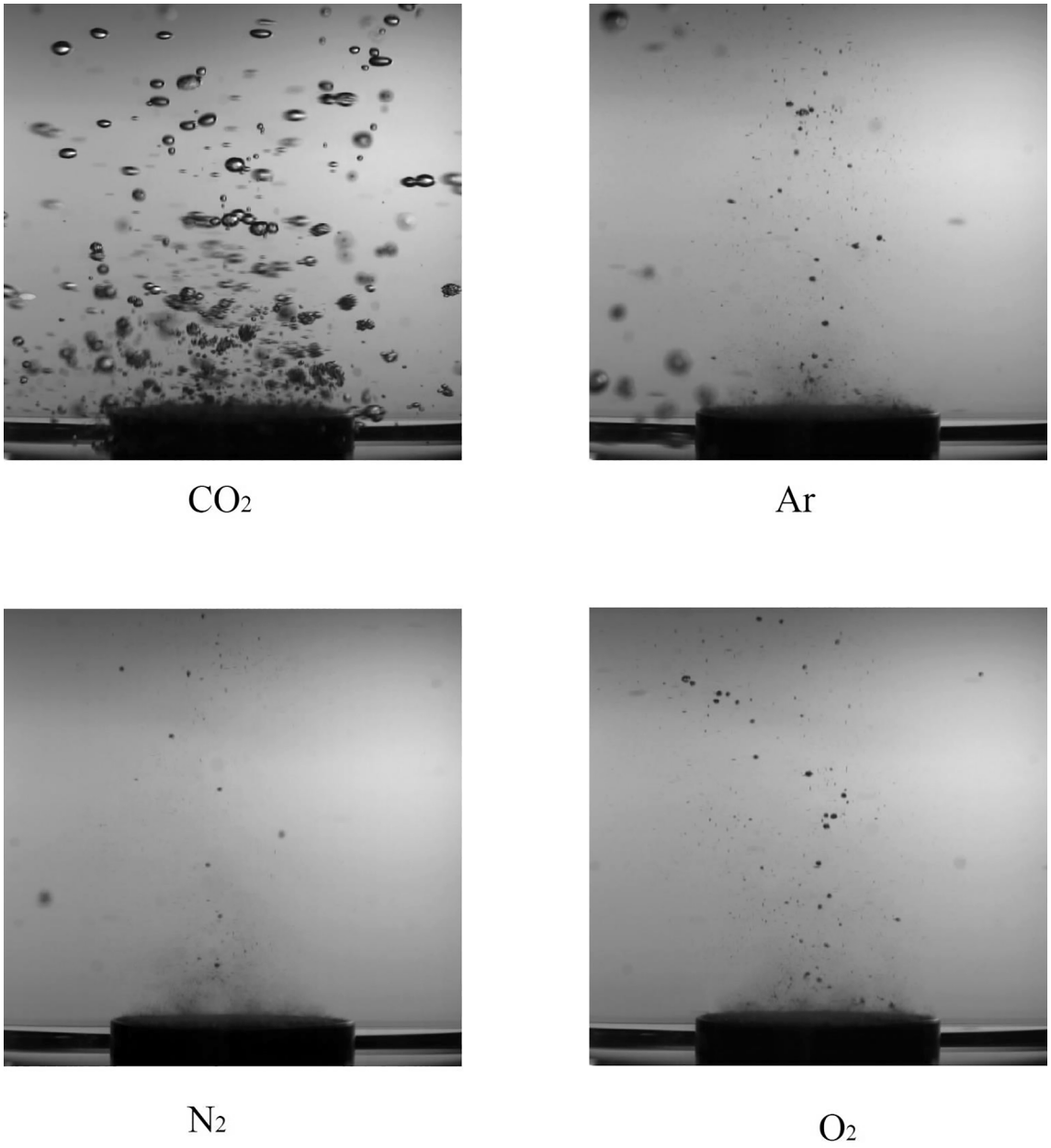

Fig. 5. High-speed camera (Photron SA 5 model at 5,000 fps) imaging of acoustic cavitation activity in 400 mL pure water under different dissolved gases sonicated by a Sinaptec transducer (20 kHz at 50% acoustic amplitude).

images reveal that the amount of cavitation activity under Ar is much higher than under N_2, which is equivalent to higher number density of acoustic cavitation bubbles and hence, higher production of hydrogen in accordance with the previous numerical findings. These observations are in perfect agreement with those of Gielen *et al.* [30], and support the aforementioned theoretical discussion.

4. Conclusions

The fallacy of causality relationship when interpreting the role of dissolved gas may wrongly lead to surprising effects when non-rational hypotheses are adopted. Thus, assumptions and methodologies need to be questioned before any "unexpected" effect is claimed. The results of some recent numerical works attributing surprising outcomes to the use of pure CO_2 as a saturation gas, in regards to the sonochemical production of hydrogen, are mostly due to failures in the modeling and simulation procedure as demonstrated through modeling and simulation in the present opinion paper. A rigorous modeling methodology should account for some facts listed hereafter:

- The single acoustic cavitation bubble is not a controlled temperature reactor, only macroscopic operating parameters can be controlled, namely acoustic and surrounding medium conditions.
- The bubble collapse, which is the seat of the sonochemical reactions, is a quasi-adiabatic phase. Temperature variation during this phase as well as its duration under the considered acoustic frequency should be respected when approaching the sonochemical reaction. It is not acceptable to simulate reactions over time longer than the collapse timeframe while adopting isothermal conditions, the assimilation of such an approach to the chemical events occurring within the bubble volume during collapse is completely dissuasive.
- From a mechanistic point of view, Argon as an inert gas, only intervenes as a third body in the reaction scheme, whilst CO_2, O_2 and

N_2 which are not inert, in addition of acting as third bodies, would disintegrate and contribute to the formation of emerging species.

- Saturation with a given gas implies particular initial conditions of bubble composition in terms of volume, these conditions are intrinsic to the gas molecule and hence, being realistic imposes to rigorously define the initial bubble composition.
- The nature of the formed acoustic cavitation under a given saturating gas, owing to its solubility, may result in bubble population phenomena such as degasification that would prevent the achievement of the sonochemical activity and hence the sonochemical production of hydrogen, this is for instance the case with CO_2.

CRediT authorship contribution statement

Kaouther Kerboua: Conceptualization, Methodology, Software, Formal analysis, Writing - original draft, Writing - review & editing. **Slimane Merouani:** Methodology, Software, Formal analysis, Writing - review & editing. **Oualid Hamdaoui:** Conceptualization, Project administration, Supervision, Visualization, Writing - review & editing. **Abdulaziz Alghyamah:** Validation, Visualization, Writing - review & editing. **Md.H. Islam:** Investigation, Writing - review & editing. **Henrik E. Hansen:** Investigation, Resources. **Bruno G. Pollet:** Conceptualization, Supervision, Visualization, Writing - review & editing.

Declaration of Competing Interest

The authors declare that they have no known competing financial interests or personal relationships that could have appeared to influence the work reported in this paper.

Acknowledgements

The authors extend their appreciation to the Deanship of Scientific Research at King Saud University for funding this work through research group No. RG-1441-501. The authors would like to thank David R. Emberson from the Combustion Kinetics Group, Department of Energy and Process Engineering, Faculty of Engineering, NTNU for setting up and filming the cavitation bubbles under sonication.

References

[1] K. Kerboua, O. Hamdaoui, Sonochemistry in Green Processes: Modeling, Experiments, and Technology, in: Sustain. Green Chem. Process. Their Allied Appl., 2020: pp. 409–460. doi:10.1007/978-3-030-42284-4.
[2] W. Lauterborn, R. Mettin, Acoustic cavitation: Bubble dynamics in high-power ultrasonic fields, Elsevier Ltd. (2015), https://doi.org/10.1016/B978-1-78242-028-6.00003-X.
[3] K. Yasui, Fundamentals of Acoustic Cavitation and Sonochemistry, in: Theor. Exp. Sonochemistry Involv. Inorg. Syst., National Institute of Advanced Industrial Science and Technology, Anagahora-Japan, 2011: pp. 1–29. doi: 10.1007/978-90-481-3887-6.
[4] T. Thanh Nguyen, Y. Asakura, S. Koda, K. Yasuda, Dependence of cavitation, chemical effect, and mechanical effect thresholds on ultrasonic frequency, Ultrason. Sonochem. 39 (2017) 301–306, https://doi.org/10.1016/j.ultsonch.2017.04.037.
[5] S.S. Rashwan, I. Dincer, A. Mohany, An investigation of ultrasonic based hydrogen production, Energy 205 (2020) 118006, https://doi.org/10.1016/j.energy.2020.118006.
[6] S.S. Rashwan, I. Dincer, A. Mohany, A unique study on the effect of dissolved gases and bubble temperatures on the ultrasonic hydrogen (sonohydrogen) production, Int. J. Hydrogen Energy 45 (41) (2020) 20808–20819, https://doi.org/10.1016/j.ijhydene.2020.05.022.
[7] K. Yasui, T. Tuziuti, J. Lee, T. Kozuka, A. Towata, Y. Iida, The range of ambient radius for an active bubble in sonoluminescence and sonochemical reactions, J. Chem. Phys. 128 (18) (2008) 184705, https://doi.org/10.1063/1.2919119.
[8] S. Merouani, O. Hamdaoui, S.M. Al-Zahrani, Toward understanding the mechanism of pure CO 2 -quenching sonochemical processes, J. Chem. Technol. Biotechnol. 95 (3) (2020) 553–566, https://doi.org/10.1002/jctb.6227.
[9] O. Authier, H. Ouhabaz, S. Bedogni, Modeling of sonochemistry in water in the presence of dissolved carbon dioxide, Ultrason. Sonochem. 45 (2018) 17–28, https://doi.org/10.1016/j.ultsonch.2018.02.044.
[10] S. Gireesan, A.B. Pandit, Modeling the effect of carbon-dioxide gas on cavitation, Ultrason. Sonochem. 34 (2017) 721–728, https://doi.org/10.1016/j.ultsonch.2016.07.005.
[11] K. Kerboua, O. Hamdaoui, Ultrasonic waveform upshot on mass variation within single cavitation bubble: Investigation of physical and chemical transformations, Ultrason. Sonochem. 42 (2018) 508–516, https://doi.org/10.1016/j.ultsonch.2017.12.015.
[12] K. Kerboua, O. Hamdaoui, Influence of reactions heats on variation of radius, temperature, pressure and chemical species amounts within a single acoustic cavitation bubble, Ultrason. Sonochem. 41 (2018) 449–457, https://doi.org/10.1016/j.ultsonch.2017.10.001.
[13] B.E. Poling, J.M. Prausnitz, J.P. O'Connel, The properties of gases and liquids, 2004. doi:10.1300/J111v23n03_01.
[14] N.A. Lange, Lange's Handbook of Chemistry, 16th ed., McGraw Hill, 1934.
[15] T.G. Leighton, 9 The principles of cavitation, Ultrasound Food Proc. (1998) 151–182, http://books.google.com/books?hl=en&lr=&id=eyCB2vJQA9cC&oi=fnd&pg=PA151&dq=the+principles+of+cavitation&ots=RJ0NOVgCLz&sig=Bs9895CIRCVGIj2CIuDgWzhungA%5Cnhttp://books.google.com/books?hl=en&lr=&id=eyCB2vJQA9cC&oi=fnd&pg=PA151&dq=9+The+principles+of+cavita.
[16] K. Yasui, Alternative model of single bubble sonoluminescence, Phys. Rev. E 56 (1997) 6750–6760, https://doi.org/10.1103/PhysRevA.65.054304.
[17] M. Kohno, T. Mokudai, T. Ozawa, Y. Niwano, Free radical formation from sonolysis of water in the presence of different gases, J. Clin. Biochem. Nutr. 49 (2) (2011) 96–101, https://doi.org/10.3164/jcbn.10-130.
[18] K. Yasui, T. Tuziuti, M. Sivakumar, Y. Iida, Theoretical study of single-bubble sonochemistry, J. Chem. Phys. 122 (22) (2005) 224706, https://doi.org/10.1063/1.1925607.
[19] E.L. Mead, R.G. Sutherland, R.E. Verrall, The effect of ultrasound on water in the presence of dissolved gases, Can. J. Chem. 54 (7) (1976) 1114–1120, https://doi.org/10.1139/v76-159.
[20] S. Merouani, O. Hamdaoui, Y. Rezgui, M. Guemini, Sensitivity of free radicals production in acoustically driven bubble to the ultrasonic frequency and nature of dissolved gases, Ultrason. Sonochem. 22 (2015) 41–50, https://doi.org/10.1016/j.ultsonch.2014.07.011.
[21] K. Yasui, T. Tuziuti, Y. Iida, H. Mitome, Theoretical study of the ambient-pressure dependence of sonochemical reactions, J. Chem. Phys. 119 (1) (2003) 346–356, https://doi.org/10.1063/1.1576375.
[22] D.G. Wayment, D.J. Casadonte Jr., Frequency effect on the sonochemical remediation of alachlor, Ultrason. Sonochem. 9 (5) (2002) 251–257, https://doi.org/10.1016/S1350-4177(02)00081-0.
[23] O. Louisnard, J. González-garcía, Acoustic Cavitation, in: Ultrasound Technol. Food Bioprocess., 2011: pp. 13–65. doi:10.1007/978-1-4419-7472-3.
[24] A. Henglein, Sonochemistry: Historical developments and modern aspects, Ultrasonics 25 (1) (1987) 6–16, https://doi.org/10.1016/0041-624X(87)90003-5.
[25] A. Henglein, Sonolysis of Carbon Dioxide, Nitrous Oxide and Methane in Aqueous Solution, Zeitschrift Für Naturforsch. B. 40 (2015) 100–107. doi:10.1515/znb-1985-0119.
[26] H. Harada, C. Hosoki, M. Ishikane, Sonophotocatalysis of water in a CO2 – Ar atmosphere, J. Photochem. Photobiol., A 160 (1-2) (2003) 11–17, https://doi.org/10.1016/S1010-6030(03)00214-4.
[27] H. Harada, Sonochemical reduction of carbon dioxide, Ultrason. Sonochem. 5 (2) (1998) 73–77, https://doi.org/10.1016/S1350-4177(98)00015-7.
[28] H. Harada, Y. Ono, Improvement of the rate of sono-oxidation in the presence of CO2, Jpn. J. Appl. Phys. 54 (2015) 52–55. doi:10.7567/JJAP.54.07HE10.
[29] J. Rooze, E.V. Rebrov, J.C. Schouten, J.T.F. Keurentjes, Effect of resonance frequency, power input, and saturation gas type on the oxidation efficiency of an ultrasound horn, Ultrason. Sonochem. 18 (1) (2011) 209–215, https://doi.org/10.1016/j.ultsonch.2010.05.007.
[30] B. Gielen, S. Marchal, J. Jordens, L.C.J. Thomassen, L. Braeken, T. Van Gerven, Influence of dissolved gases on sonochemistry and sonoluminescence in a flow reactor, Ultrason. Sonochem. 31 (2016) 463–472, https://doi.org/10.1016/j.ultsonch.2016.02.001.